

MedChemComm

Accepted Manuscript



This is an *Accepted Manuscript*, which has been through the Royal Society of Chemistry peer review process and has been accepted for publication.

Accepted Manuscripts are published online shortly after acceptance, before technical editing, formatting and proof reading. Using this free service, authors can make their results available to the community, in citable form, before we publish the edited article. We will replace this *Accepted Manuscript* with the edited and formatted *Advance Article* as soon as it is available.

You can find more information about *Accepted Manuscripts* in the [Information for Authors](#).

Please note that technical editing may introduce minor changes to the text and/or graphics, which may alter content. The journal's standard [Terms & Conditions](#) and the [Ethical guidelines](#) still apply. In no event shall the Royal Society of Chemistry be held responsible for any errors or omissions in this *Accepted Manuscript* or any consequences arising from the use of any information it contains.

2-Pyridylquinolone Antimalarials with Improved Antimalarial Activity and Physicochemical Properties

Sitthivut Charoensutthivarakul,^a W. David Hong,^a Suet C. Leung,^a Peter D. Gibbons,^a Paul T.P. Bedingfield,^b Gemma L. Nixon,^a Alexandre S. Lawrenson,^a Neil G. Berry,^a Stephen A. Ward,^b Giancarlo A. Biagini^b and Paul M. O'Neill*^a

A series of 2-pyridylquinolones has been prepared in 5-7 steps and through lead optimisation, antimalarial activity as low as 12 nM against *Plasmodium falciparum* (*Pf*) has been achieved. Compared with previous analogues in this series, selected molecules have improved solubility, a reduced potential for off-target toxicity and improved metabolic stability profiles. Docking studies performed with a homology model of the *Pfbc*₁ complex target demonstrate a key role for the Tyr16 residues in the recognition of highly active quinolone based inhibitors.

Introduction

Malaria is caused by parasites of the genus *Plasmodium* which are widespread in tropical and subtropical regions of the world and is responsible for one million deaths every year¹. *Plasmodium falciparum* is the most deadly form of the parasite transmitted to the human host by *Anopheles* mosquitoes² and has developed resistance to many of the established classes of drugs³. Due to drug resistance, the discovery of novel drug candidates remains a top priority. The development of compounds focused on hitting new targets is seen as a viable way forward and is an established approach to avoid cross resistance with available antimalarials⁴.

There are a large number of recent studies based on the development of antimalarials with quinolone-related structures⁵⁻⁷. One of these programmes resulted in the discovery of ELQ-300, a selective cytochrome *bc*₁ inhibitor now in pre-clinical development⁸⁻¹⁰. Our recent work has shown that inhibition of two mitochondrial enzymes in the electron transport chain – the cytochrome *bc*₁ complex and the recently identified *Pf*NDH2 (Type II NADH:ubiquinone oxidoreductase)^{11, 12} – results in the collapse of the mitochondrial membrane potential and to the inhibition of *de novo* pyrimidine biosynthesis and ultimately parasite death¹³. Since effective dual inhibition of these proteins can be observed with the 2-aryl and 2-pyridylquinolone pharmacophore^{14a} a number of inhibitors based on this structure have been identified. Two such lead compounds are **CK-2-68** and **SL-2-25 (1)** – both of which confer potent nanomolar activity against asexual and liver stages of *P. falciparum*^{15, 16} (**Figure 1**). Here, we describe further modifications of the quinolone A-ring and 2-pyridyl side chain with the aim of reducing lipophilicity in an attempt to provide compounds with improved activity/solubility profiles.

In order to increase polarity of our quinolone hit series we incorporated a hydroxyl group into the A-ring at one of the 6, 7 or 8-positions. The inclusion of the hydroxyl group in the quinolone A-ring offered the option of exploring pro-drugs for the series by derivatisation to provide either phosphate or carbamate pro-drugs. Since the corresponding methoxy analogues were prepared *en route* to **23 - 25**, these compounds were also screened against *Plasmodium falciparum*.

Results and discussion

The synthesis of the methoxy and hydroxy series was accomplished in 5-7 steps from commercially available starting materials (see **Scheme 1**). Aldehyde **2**, synthesised from corresponding boronic acid and aromatic halide in excellent yield (see supporting information), was utilised in a Grignard reaction to give alcohol **3** in 32-83% yields. Alcohol **3** was then oxidised using PCC to yield ketone **4** in good yields. Oxazole **6** was prepared in yields of 31-98% from the respective isatoic anhydride **5** which was synthesised by adding diphosgene into methoxy-substituted anthranilic acid¹⁷ (see Supporting information). Reaction of oxazole **6** with ketone **4** in the presence of catalytic trifluoromethane sulfonic acid gave the desired quinolones **7 - 22** in 4-62% yields¹⁸. Some selected quinolones were further demethylated by adding BBr₃ to obtain hydroxyl analogues **23-25** in 10-69 % yields.

From previous work, we had identified the *p*-OCF₃ substituent on the D-ring provided excellent antimalarial activity. More recent work within our group on a related quinolone series revealed some advantages in 3,4-dichloro substitution (**Figure 2**) and for this reason we also briefly investigated this substitution pattern within the quinolone D-ring side-chain in analogues **16-17**.

Antimalarial activities

Analysis of the *in vitro* data reveals that excellent activity can be achieved by the introduction of a methoxyl group in the 7-position (see **Table 2**, entries **9**, **11** and **13**). A clear trend is seen in the pyridyl series where 7-methoxy analogues provide optimal activity (see for example direct comparison of **SL-2-25** and **9**). In contrast, 5, 6 and 8-methoxy analogues of **SL-2-25** resulted in a complete loss in antimalarial activity.

Hydroxyl substitution is less favorable when compared with their methoxylated products (see **Table 2**, for example comparison between **9** and **24**). Some regioisomers of **9** (eg. **11** and **13**) exhibit potent activity against the parasite. 3,4-Dichlorophenyl substitution also is tolerated as seen in **17** and **22** both of which show excellent antimalarial efficacy. Although 7-methoxy analogues provide the best activity, we also noted that analogues **18**, **20** and **22**, which lack this substituent, are potent nanomolar antimalarials.

Looking into their molecular structures, compound **9**, **15**, **16**, and **21** containing a 7-OMe group and a similar *para* substitution side chain devoid of flexibility show low to moderate antimalarial activities. On the other hand, **11 - 14** and **17 - 20** containing *meta* substitution configured side chains exhibit good to outstanding efficacy against the 3D7 parasite strain.

Additionally, some selected compounds were tested against drug resistant strains of *P. falciparum* including chloroquine resistant W2 and atovaquone resistant TM90C2B (**Table 3**). Compound **11** and **13**, both contain flexible side chains, showed excellent activities against both W2 and TM90C2B strains that are comparable to marketed drugs (chloroquine and atovaquone) and **SL-2-25**. Notably, against the atovaquone resistant strain TM90C2B both **11** and **13** express excellent activity and show no cross resistance with atovaquone. Both **11** and **13** were also tested against 3D7-yDHODH-GFP, a transgenic derivative of *P. falciparum* 3D7 containing yeast dihydroorotate dehydrogenase,^{14a,b} and were shown to be inactive (IC₅₀ >1 μM), consistent with these inhibitors targeting the electron transport chain of the parasite mitochondria.

Drug Solubility Profiles

The poor aqueous solubility associated with the 2- and 3-aryl/pyridyl quinolone series of antimalarial provides development challenges for this class of drug. Previous research indicates that quinolones generally have poor aqueous solubility due to planar aggregation via π -stacking of their ring system¹⁶. This interaction also leads to higher observed melting points¹⁹. Several strategies can be used to improve the solubility; here, we explored the incorporation of a polar head group with modification of the pyridyl side-chain geometry. For those derivatives expressing higher potency, a 96-well plate aqueous solubility assessment was performed¹⁹. The results are shown in **Table 4**. A clear relationship between melting point and solubility was observed. Compound **18** had the best aqueous solubility amongst the selected quinolones that correlated with its low melting point. Although 3,4-dichlorophenyl analogues (**16**, **17** and **22**) gave excellent activity, it is worth noting that a high melting point is observed which possibly reflects a decrease in aqueous solubility. Inspection of the side chain suggests that the pyridyl function exclusively affects both antimalarial activity and solubility. The presence of the pyridyl substitution (3,5-disubstituted pyridyl) as in **11**, **17** and **18** gives excellent potency and a range of melting points that were significantly lower than **SL-2-25**'s. This relationship can be used within this compound class to compare solubility.

Metabolic Stability Profiles

Selected potent quinolones were also profiled in microsomal stability assessment in human liver microsomes and rat hepatocytes. Human microsomal stability assessment shows how stable the drug is when enters CYP450 oxidation stage, while rat hepatocytic clearance shows the compound stability in both phase I and phase II metabolism²⁰. Comparing 7-OMe (**11** and **17**) to 7-H (**18**, **20**, **22**) analogues, 7-OMe compounds are more sensitive to CYP450 turnover, possibly as a result of 7-*O*-demethylation. 3,4-Dichlorophenyl compounds (**17**, **22**) are more stable in human microsomal media than their *p*-OCF₃ counterparts; the reverse is seen in rat hepatocytes with greater stability observed for the latter *p*-substituent.

Potential for Off-target *bc*₁ Inhibition

Previous antimalarial projects that have focused on the development of *bc*₁ inhibitors have had to be terminated because of safety concerns regarding cardiotoxicity²¹. Therefore, a bovine *bc*₁ counterscreen was established to investigate potential mammalian mitochondrial toxicity²². Some highly potent compounds were assessed *in vitro*, using bovine heart *bc*₁ inhibition as displayed in **Table 6**.

The single-point inhibition experiments were run at two different concentrations of select compounds – 100 nM and 1 μ M. A low % inhibition represents that the compound is less active in the bovine heart *bc*₁ screen. There is no obvious trend when comparing 7-H compounds to their 7-OMe counterparts. Generally, the substitutions on pyridyl ring as in **11**, **17** and **18** provide molecules with lower affinity for the mammalian *bc*₁ target. Further studies are required to examine how this relationships extends to human heart tissue derived isolated *bc*₁ complexes.

Molecular Modeling

We have recently shown that 4-(1H)-pyridones bind to the Q_i site in cytochrome *bc*₁.²³ Consequently molecular modeling studies were undertaken to provide insight as to how the compounds bind to this site. Shown in Figure 3 is the docking pose between **9** and a *Plasmodium* homology model of the yeast *bc*₁ complex.

A homology model of cytochrome *bc*₁ based on the primary sequence Q02768 and the 1NTK *B. taurus* *bc*₁ complex template was created with the PHYRE online homology modelling tool²⁴. The model was used to predict the binding of **9** within the Q_i active site.

Using GOLD and the methods developed in our group²⁵ compounds were docked into the binding site. We observed that our potent inhibitors, **9** and **17**, were predicted to bind tightly to the Q_i site with the average PLP scores of 64 and 61, respectively.

In line with previous *bc*₁ crystal structures with molecules bound in the Q_i site (GW844520, GSK932121²³, antimycin or NQNO²⁶), it was found that the interaction of quinolones with the *bc*₁ target also involved several interactions – polar and hydrophobic. These include a hydrogen bond between Asp218 and the quinolone's NH group whilst there is another weak hydrogen bond between Ser196 and the carbonyl group, very similar to the interactions of GW844520, GSK932121²³ and antimycin.²⁶ Of particular importance is the hydrophobic interaction of 7-methoxy within a hydrophobic pocket created by Leu214, Ile22, Phe210 and Trp26. The pyridyl group of **9** forms π stacking interactions with Phe30 and His12 whilst the OCF₃ moiety appears to form hydrophobic contacts with Ile34 and Phe37, which is similar to the interaction of the pentyl moiety in antimycin and alkyl chain in NQNO with the same two residues. This latter interaction is likely to be an important factor in providing extra levels of antimalarial activity as seen for **9**, **11**, **13** and **17**.

Conclusion

A 5-7 step synthesis of an array of 2-pyridylquinolones with potent antimalarial activity has been described. Subtle changes to the geometry of the side chain have a profound effect on the inherent antimalarial activity, physicochemical, metabolic and *bc*₁

inhibitory profiles of related quinolone analogues. In terms of balance of properties, analogues **17** and **18** have improved properties over the initial lead compound with a reduced propensity for off-target mammalian bc_1 inhibition coupled with improved solubility/ metabolic stability. These observations encourage selection of molecules in this class for additional *in vivo* PK and mouse activity assessment in the near future.

Experimental

Air- and moisture-sensitive reactions were carried out in oven-dried glassware, sealed with rubber septa, under nitrogen from a balloon. Air- and moisture-sensitive liquids and reagents were transferred via syringe. Reactions were stirred using Teflon-coated magnetic stir bars. All commercial reagents were used without further purifications. NMR spectra were recorded in $CDCl_3$ or $DMSO-d_6$ on a Bruker AMX400 spectrometer (1H 400 MHz, ^{13}C 100 MHz). Chemical shifts (δ) were expressed in ppm relative to tetramethylsilane (TMS) as an internal standard. J values are in hertz (Hz) and the splitting patterns were designed as follows: s, singlet; d, doublet; t, triplet; q, quartet; dd, double doublet; m, multiplet. Mass spectra were recorded on either a Micromass LCT Mass Spectrometer using electrospray ionisation (ESI) or Trio-1000 Mass Spectrometer using chemical ionisation (CI). Elemental analysis (%C, %H, %N) was performed in the University of Liverpool microanalysis laboratory. All melting points were determined with Gallenkamp melting point apparatus and were uncorrected. See supporting information for experimental and data on all intermediates.

General procedure for the synthesis of quinolones

To a solution of *o*-oxazoline-substituted anilines (1.1 eq, 1.1 mmol) and ketones (1.0 eq, 1.0 mmol) in dry *n*-butanol (15 mL) was added trifluoromethane sulfonic acid (20 mol %) and the mixture was stirred under reflux (135 °C) for 24 hours. The reaction was cooled to room temperature and the solvent was evaporated under vacuum. Saturated sodium carbonate solution (20 mL) was added. The aqueous solution was extracted with EtOAc (3 x 20 mL), washed with brine, dried over $MgSO_4$, and concentrated under vacuum. The crude mixture was purified by column chromatography to give quinolones.

9: white solid (yield 51%); mp 324 -325 °C; 1H NMR (400 MHz, $DMSO$) δ 11.60 (s, 1H, NH), 8.88 (d, J = 1.9 Hz, 1H), 8.34 (d, J = 8.8 Hz, 2H), 8.24 (d, J = 8.2 Hz, 1H), 8.15 (dd, J = 8.2, 1.9 Hz, 1H), 8.04 (d, J = 9.0 Hz, 1H), 7.55 (d, J = 8.8 Hz, 2H), 6.99 (d, J = 2.3 Hz, 1H), 6.93 (dd, J = 9.0, 2.3 Hz, 1H), 3.84 (s, 3H, 7-OMe), 1.93 (s, 3H, 3-Me). ^{13}C NMR (101 MHz, $DMSO$) δ 162.1, 155.4, 149.8, 138.5, 130.3, 129.2, 129.1, 121.7, 121.6, 120.4, 118.0, 115.2, 113.6, 99.0, 55.7, 12.3. ES HRMS: m/z calculated for $C_{23}H_{18}N_2O_3F_3$ ($[M+H]^+$) 427.127, found 427.129.

11: white solid (yield 34%); mp 255 -258 °C; 1H NMR (400 MHz, $DMSO$) δ 11.57 (s, 1H, NH), 9.10 (d, J = 2.2 Hz, 1H), 8.80 (d, J = 2.2 Hz, 1H), 8.35 (t, J = 2.2 Hz, 1H), 8.05 (d, J = 9.0 Hz, 1H), 8.01 (d, J = 7.9 Hz, 2H), 7.55 (d, J = 7.9 Hz, 2H), 6.97 (d, J = 2.3 Hz, 1H), 6.93 (dd, J = 9.0, 2.3 Hz, 1H), 3.84 (s, 3H, 7-OMe), 1.94 (s, 3H, 3-Me). ^{13}C NMR (101 MHz, $DMSO$) δ 176.6, 162.1, 148.9, 148.7, 144.2, 141.7, 136.1, 135.1, 134.3, 131.4, 129.6, 127.3, 122.1, 118.1, 115.3, 113.6, 99.0, 55.7, 12.3. ESI HRMS: m/z calculated for $C_{23}H_{18}N_2O_3F_3$ ($[M+H]^+$) 427.127, found 427.127.

13: white solid (yield 34%); mp 245 -247 °C; 1H NMR (400 MHz, $DMSO$) δ 11.56 (s, 1H, NH), 8.89 (d, J = 5.0 Hz, 1H), 8.34 (d, J = 8.0 Hz, 2H), 8.22 (br s, 1H), 8.06 (d, J = 9.0 Hz, 1H), 7.60 (dd, J = 5.0, 1.5 Hz, 1H), 7.53 (d, J = 8.0 Hz, 2H), 7.00 (d, J = 2.4 Hz, 1H), 6.94 (dd, J = 9.0, 2.4 Hz, 1H), 3.85 (s, 3H, 7-OMe), 1.93 (s, 3H, 3-Me). ^{13}C NMR (101 MHz, $DMSO$) δ 176.6, 162.1, 155.5, 150.4, 144.9, 144.2, 141.7, 137.7, 129.2, 127.3, 123.2, 121.6, 120.7, 118.1, 114.7, 113.7, 111.4, 99.1, 55.7, 12.2. ESI HRMS: m/z calculated for $C_{23}H_{18}N_2O_3F_3$ ($[M+H]^+$) 427.127, found 427.127.

17: yellow solid (yield 17%); mp 290 -292 °C; 1H NMR (400 MHz, $DMSO$) δ 11.59 (s, 1H, NH), 9.15 (d, J = 2.0 Hz, 1H), 8.81 (d, J = 2.0 Hz, 1H), 8.43 (t, J = 2.0 Hz, 1H), 8.22 (d, J = 2.2 Hz, 1H), 8.05 (d, J = 8.9 Hz, 1H), 7.91 (dd, J = 8.5, 2.2 Hz, 1H), 7.82 (d, J = 8.5 Hz, 1H), 6.98 (d, J = 2.4 Hz, 1H), 6.94 (dd, J = 8.9, 2.4 Hz, 1H), 3.85 (s, 3H, 7-OMe), 1.93 (s, 3H, 3-Me). ESI HRMS: m/z calculated for $C_{22}H_{16}O_2^{35}Cl_2$ ($[M+H]^+$) 411.067, found 411.067.

18: pale yellow solid (yield 54%); mp 217 - 220 °C; 1H NMR (400 MHz, $DMSO$) δ 11.77 (s, 1H, NH), 9.12 (d, J = 2.1 Hz, 1H), 8.82 (d, J = 2.1 Hz, 1H), 8.38 (t, J = 2.1 Hz, 1H), 8.16 (dd, J = 8.3, 1.2 Hz, 1H), 8.01 (d, J = 8.8 Hz, 2H), 7.66 (ddd, J = 8.3, 6.9, 1.5 Hz, 1H), 7.59 (d, J = 7.9 Hz, 1H), 7.56 (d, J = 8.8 Hz, 2H), 7.34 (ddd, J = 7.9, 6.9, 1.2 Hz, 1H), 1.96 (s, 3H, 3-Me). ^{13}C NMR (101 MHz, $DMSO$) δ 177.0, 148.9, 148.7, 144.7, 139.9, 136.0, 135.2, 134.2, 131.9, 131.4, 129.6, 125.4, 123.5, 123.3, 122.1, 118.5, 115.6, 12.4. ESI HRMS: m/z calculated for $C_{22}H_{16}N_2O_3F_3$ ($[M+H]^+$) 397.116, found 397.117.

20: off-white solid (yield 56%); mp 244 - 246 °C; 1H NMR (400 MHz, $DMSO$) δ 11.78 (s, 1H, NH), 8.90 (dd, J = 4.9, 0.7 Hz, 1H), 8.35 (d, J = 8.9 Hz, 2H), 8.26 (br s, 1H), 8.16 (dd, J = 8.2, 1.1 Hz, 1H), 7.67 (ddd, J = 8.2, 6.8, 1.5 Hz, 1H), 7.63 (dd, J = 4.9, 1.5 Hz, 1H), 7.60 (d, J = 7.8 Hz, 1H), 7.53 (d, J = 8.9 Hz, 2H), 7.34 (ddd, J = 7.8, 6.8, 1.1 Hz, 1H), 1.95 (s, 3H, 3-Me). ^{13}C NMR (101 MHz, $DMSO$) δ 150.4, 144.1, 139.9, 131.9, 129.2, 125.4, 123.5, 123.3, 123.3, 123.2, 121.6, 120.7, 118.6, 115.0, 12.3. ESI HRMS: m/z calculated for $C_{22}H_{16}N_2O_3F_3$ ($[M+H]^+$) 397.116, found 397.117.

22: a pale yellow solid (yield 25%); mp = 270 - 272 °C; 1H NMR (400 MHz, $DMSO$) δ 11.75 (s, 1H, NH), 9.15 (d, J = 2.1 Hz, 1H), 8.82 (d, J = 2.1 Hz, 1H), 8.45 (t, J = 2.1 Hz, 1H), 8.22 (d, J = 2.2 Hz, 1H), 8.15 (dd, J = 8.0, 1.1 Hz, 1H), 7.91 (dd, J = 8.4,

2.2 Hz, 1H), 7.81 (d, $J = 8.4$ Hz, 1H), 7.66 (ddd, $J = 8.0, 6.9, 1.5$ Hz, 1H), 7.59 (d, $J = 8.0$ Hz, 1H), 7.33 (ddd, $J = 8.0, 6.9, 1.1$ Hz, 1H), 1.95 (s, 3H, 3-Me). HRMS (CI): m/z calculated for $C_{21}H_{14}N_2O^{35}Cl_2$ ($[M+H]^+$) 381.056, found 381.055.

Parasite Culture

Plasmodium blood stage cultures²⁷ and drug sensitivity²⁸ were determined by established methods. IC₅₀s (50% inhibitory concentrations) were calculated by using the four-parameter logistic method (Grafit program; Erithacus Software, United Kingdom).

Molecular Modeling

A homology model of *P. falciparum* cytochrome *bc*₁ complex was constructed using the PHYRE online homology modelling program²⁴. The *P. falciparum* cytochrome *b* primary sequence Q02768 was obtained from UNIPROT²⁹ used as the query sequence. A one to one threading model was built using PHYRE and the model produced had a confidence score of 100%. The docking was performed using default settings in Gold with ten docking poses calculated for each quinolone.

Acknowledgements

S.C. thanks the University of Liverpool and Mahidol University, Thailand for the financial support under the Mahidol-Liverpool Scholarship scheme. We thank Dr Denis E. Kyle (Department of Global Health, College of Public Health, University of South Florida, USA) for the antimalarial testing contained in Table 3 and AstraZeneca for metabolic stability measurements.

Notes and references

^a Department of Chemistry, University of Liverpool, Liverpool, L69 7ZD, United Kingdom.

^b Liverpool School of Tropical Medicine, Pembroke Place, Liverpool. L3 5QA, United Kingdom.

Electronic Supplementary Information (ESI) available: See DOI: 10.1039/b000000x/

1. C. J. L. Murray, L. C. Rosenfeld, S. S. Lim, K. G. Andrews, K. J. Foreman, D. Haring, N. Fullman, M. Naghavi, R. Lozano and A. D. Lopez, *The Lancet*, 2012, **379**, 413-431.
2. WHO, *World malaria report 2009*, World Health Organization, Geneva, 2009.
3. T. Rodrigues, R. Moreira and F. Lopes, *Future Medicinal Chemistry*, 2010, **3**, 1-3.
4. J. N. Burrows, K. Chibale and T. N. C. Wells, *Curr Top Med Chem*, 2011, **11**, 1226-1254.
5. R. M. Cross, D. L. Flanigan, A. Monastyrskiy, T. Mutka, D. E. Kyle and R. Manetsch, *Abstr Pap Am Chem S*, 2010, **239**.
6. R. M. Cross, A. Monastyrskiy, T. S. Mukta, J. N. Burrows, D. E. Kyle and R. Manetsch, *J Med Chem*, 2010, **53**, 7076-7094.
7. R. M. Cross, N. K. Namelikonda, T. S. Mutka, L. Luong, D. E. Kyle and R. Manetsch, *J Med Chem*, 2011, **54**, 8321-8327.
8. A. Nilsen, A. N. LaCrue, K. L. White, I. P. Forquer, R. M. Cross, J. Marfurt, M. W. Mather, M. J. Delves, D. M. Shackleford, F. E. Saenz, J. M. Morrissey, J. Steuten, T. Mutka, Y. X. Li, G. Wirjanata, E. Ryan, S. Duffy, J. X. Kelly, B. F. Sebayang, A. M. Zeeman, R. Noviyanti, R. E. Sinden, C. H. M. Kocken, R. N. Price, V. M. Avery, I. Angulo-Barturen, M. B. Jimenez-Diaz, S. Ferrer, E. Herreros, L. M. Sanz, F. J. Gamon, I. Bathurst, J. N. Burrows, P. Siegl, R. K. Guy, R. W. Winter, A. B. Vaidya, S. A. Charman, D. E. Kyle, R. Manetsch and M. K. Riscoe, *Sci Transl Med*, 2013, **5**.
9. A. Nilsen, G. P. Miley, I. P. Forquer, M. W. Mather, K. Katneni, Y. X. Li, S. Pou, A. M. Pershing, A. M. Stickles, E. Ryan, J. X. Kelly, J. S. Doggett, K. L. White, D. J. Hinrichs, R. W. Winter, S. A. Charman, L. N. Zakharov, I. Bathurst, J. N. Burrows, A. B. Vaidya and M. K. Riscoe, *J Med Chem*, 2014, **57**, 3818-3834.
10. R. Winter, J. X. Kelly, M. J. Smilkstein, D. Hinrichs, D. R. Koop and M. K. Riscoe, *Exp Parasitol*, 2011, **127**, 545-551.
11. G. A. Biagini, P. Viriyavejakul, P. M. O'Neill, P. G. Bray and S. A. Ward, *Antimicrob Agents Ch*, 2006, **50**, 1841-1851.
12. N. Fisher, P. G. Bray, S. A. Ward and G. A. Biagini, *Trends in Parasitology*, 2007, **23**, 305-310.
13. I. K. Srivastava, H. Rottenberg and A. B. Vaidya, *J Biol Chem*, 1997, **272**, 3961-3966.
14. G. A. Biagini, N. Fisher, A. E. Shone, M. A. Mubarak, A. Srivastava, A. Hill, T. Antoine, A. J. Warman, J. Davies, C. Pidathala, R. K. Amewu, S. C. Leung, R. Sharma, P. Gibbons, D. W. Hong, B. Pacorel, A. S. Lawrenson, S. Charoensutthivarakul, L. Taylor, O. Berger, A. Mbekeani, P. A. Stocks, G. L. Nixon, J. Chadwick, J. Hemingway, M. J. Delves, R. E. Sinden, A. M. Zeeman, C. H. M. Kocken, N. G. Berry, P. M. O'Neill and S. A. Ward, *P Natl Acad Sci USA*, 2012, **109**, 8298-8303.
15. S. C. Leung, P. Gibbons, R. Amewu, G. L. Nixon, C. Pidathala, W. D. Hong, B. Pacorel, N. G. Berry, R. Sharma, P. A. Stocks, A. Srivastava, A. E. Shone, S. Charoensutthivarakul, L. Taylor, O. Berger, A. Mbekeani, A. Hill, N. E. Fisher, A. J. Warman, G. A. Biagini, S. A. Ward and P. M. O'Neill, *J Med Chem*, 2012, **55**, 1844-1857.

16. C. Pidathala, R. Amewu, B. Pacorel, G. L. Nixon, P. Gibbons, W. D. Hong, S. C. Leung, N. G. Berry, R. Sharma, P. A. Stocks, A. Srivastava, A. E. Shone, S. Charoensutthivarakul, L. Taylor, O. Berger, A. Mbekeani, A. Hill, N. E. Fisher, A. J. Warman, G. A. Biagini, S. A. Ward and P. M. O'Neill, *J Med Chem*, 2012, **55**, 1831-1843.
17. R. Giri, N. Maugel, B. M. Foxman and J. Q. Yu, *Organometallics*, 2008, **27**, 1667-1670.
18. F. T. Luo, V. K. Ravi and C. H. Xue, *Tetrahedron*, 2006, **62**, 9365-9372.
19. C. A. Lipinski, F. Lombardo, B. W. Dominy and P. J. Feeney, *Advanced Drug Delivery Reviews*, 2001, **46**, 3-26.
20. J. B. Houston, *Biochemical pharmacology*, 1994, **47**, 1469-1479.
21. V. Barton, N. Fisher, G. A. Biagini, S. A. Ward and P. M. O'Neill, *Current Opinion in Chemical Biology*, 2010, **14**, 440-446.
22. G. A. Biagini, N. Fisher, N. Berry, P. A. Stocks, B. Meunier, D. P. Williams, R. Bonar-Law, P. G. Bray, A. Owen, P. M. O'Neill and S. A. Ward, *Molecular Pharmacology*, 2008, **73**, 1347-1355.
23. M. J. Capper, P. M. O'Neill, N. Fisher, R. W. Strange, D. Moss, S. A. Ward, N. G. Berry, A. S. Lawrenson, S. S. Hasnain, G. A. Biagini and S. V. Antonyuk, *Proceedings of the National Academy of Sciences of the United States of America*, 2015.
24. L. A. Kelley and M. J. E. Sternberg, *Nat Protoc*, 2009, **4**, 363-371.
25. R. Sharma, A. S. Lawrenson, N. E. Fisher, A. J. Warman, A. E. Shone, A. Hill, A. Mbekeani, C. Pidathala, R. K. Amewu, S. Leung, P. Gibbons, D. W. Hong, P. Stocks, G. L. Nixon, J. Chadwick, J. Shearer, I. Gowers, D. Cronk, S. P. Parel, P. M. O'Neill, S. A. Ward, G. A. Biagini and N. G. Berry, *J Med Chem*, 2012, **55**, 3144-3154.
26. X. Gao, X. Wen, L. Esser, B. Quinn, L. Yu, C. A. Yu and D. Xia, *Biochemistry*, 2003, **42**, 9067-9080.
27. W. Trager and J. B. Jensen, *Science*, 1976, **193**, 673-675.
28. M. Smilkstein, N. Sriwilaijaroen, J. X. Kelly, P. Wilairat and M. Riscoe, *Antimicrobial agents and chemotherapy*, 2004, **48**, 1803-1806.
29. G. Vriend, *J Mol Graphics*, 1990, **8**, 52-56.

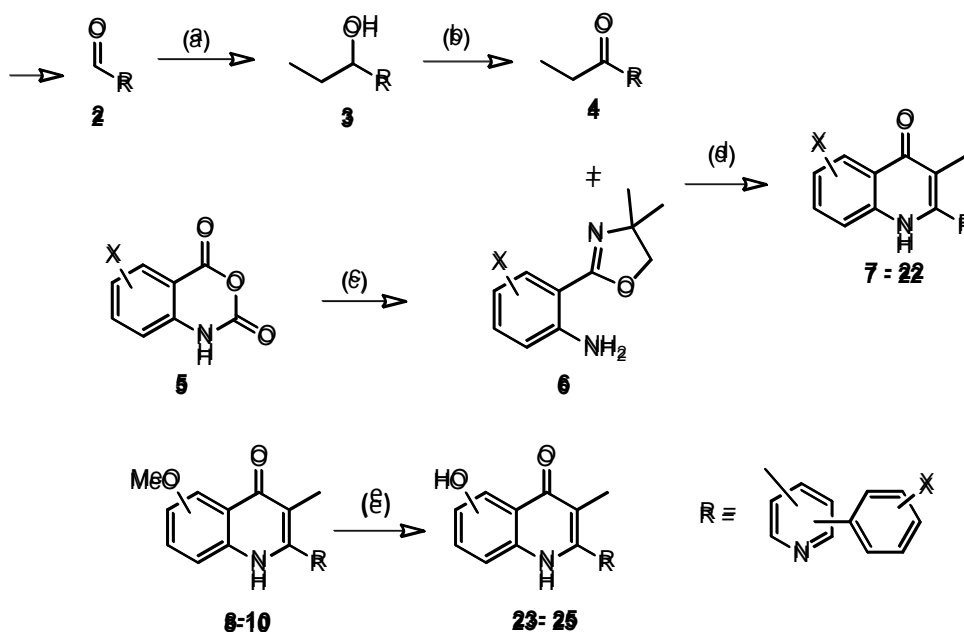
Figure Legends

Figure 1. The quinolone core structure and initial lead compounds CK-2-68 and SL-2-25 (**1**) – and their antimalarial activity

Figure 2. Previous work on 4-trifluoromethoxybenzyl and 3,4-dichlorobenzyl analogues.

Figure 3. *In silico* docking of **9** into the *Plasmodium falciparum* *bc₁* homology model. Protein rendered as a cartoon in cyan with residues rendered as sticks. **9** rendered as sticks (carbon – grey, hydrogen – white, oxygen – red, nitrogen – blue, fluorine – cyan). Hydrogen bond indicated by black dashed line with distance given in Ångstrom.

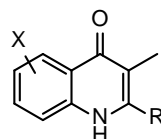
Scheme



Conditions: (a) EtMgBr, THF, 0 °C, under N₂, 1 h (b) PCC, DCM, 2 h (c) 2-amino-2-methyl-propanol, ZnCl₂, PhCl, 135 °C (d) CF₃SO₃H, *n*-BuOH, under N₂, 130 °C, 24 h (e) BBr₃, DCM, rt., overnight.

Scheme 1. Synthesis of Quinolones.

Tables

**Table 1** Yields for the synthesis of quinolone 7-22.

Compound	R	X	No. of steps	% Yield 3	% Yield 4	% Yield 6	% Yield 7-22
7		5-OMe	6	67	69	98	4
8		6-OMe	6	67	69	48	22
9		7-OMe	6	67	69	73	51
10		8-OMe	6	67	69	30	25
11		7-OMe	6	32	92	73	34
12		7-OMe	6	73	47	73	40
13		7-OMe	6	55	99	73	34
14		7-OMe	7	32	66	73	42
15		7-OMe	6	37	97	73	62
16		7-OMe	6	83	69	73	23
17		7-OMe	6	65	33	73	17
18		7-H	5	32	92	31	54
19		7-H	5	73	47	31	55
20		7-H	5	55	99	31	56
21		7-H	5	37	97	31	62
22		7-H	5	65	33	31	25

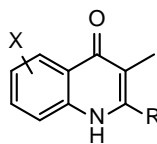


Table 2 In vitro antimalarial Activities versus 3D7 *P. falciparum* , aqueous solubilities and melting points of quinolones

Compound	R	X	IC ₅₀ (nM) 3D7 ± SD	Melting point
SL-2-25		7-H	54 ± 6	277 - 278 °C
7		5-OMe	> 1000	ND
8		6-OMe	> 1000	312 - 314 °C
9		7-OMe	14 ± 2	324 - 325 °C
10		8-OMe	> 1000	182 - 185 °C
11		7-OMe	12 ± 3	255-258 °C
12		7-OMe	149 ± 5	200-204 °C
13		7-OMe	12 ± 3	245-247 °C
14		7-OMe	150 ± 10	188-190 °C
15		7-OMe	> 1000	255-258 °C
16		7-OMe	200 ± 10	268-270 °C
17		7-OMe	18 ± 3	290-292 °C
18		7-H	41 ± 2	217-220 °C
19		7-H	390 ± 30	187-192 °C
20		7-H	21 ± 5	244-246 °C
21		7-H	> 1000	239-241 °C
22		7-H	40 ± 4	270-272 °C
23		6-OH	326 ± 50	decomposed at 250°C
24		7-OH	202 ± 79	ND
25		8-OH	> 1000	154 - 156 °C

Table 3. Drug resistant parasites inhibition profiles of selected quinolones

Compound	IC ₅₀ (nM)	IC ₅₀ (nM)
	W2	TM90C2B
chloroquine	12.3	14.5
atovaquone	0.3	9908
SL-2-25	48	156
11	4.0	7.2
13	4.2	7.0

Table 4. Selected compounds solubility profiles

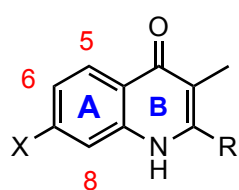
Compound	Melting point	Kinetic Solubility	
		(μM)	
		pH 1	pH 7.4
SL-2-25	277 - 278 °C	3.2	<1
9	324 -325 °C	2.6	<1
11	255 -258 °C	7.8	<1
13	245 -247 °C	120	<1
17	290 -292 °C	15	14
18	217 -220 °C	140	3.6
20	244 -246 °C	79	2.1

Table 5. Selected compounds metabolic stability profiles

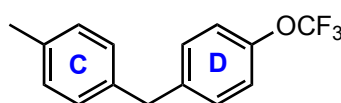
Compound	Human Mics CL _{int}	Rat Heps CL _{int}
	(μL/min/mg)	(μL/min/10 ⁶ cell)
SL-2-25	20.6	ND
11	25.9	1.2
17	14	4.9
18	12.5	1.8
20	7.7	2.5
22	5.6	9.9

Table 6. Enzyme and parasite inhibition profiles of selected quinolones.

Compound	IC ₅₀ (nM) 3D7	Bovine heart <i>bc</i> ₁	Bovine heart <i>bc</i> ₁
		(% inhibition at 100 nM)	(% inhibition at 1 μM)
9	14	55	98
11	12	19	81
13	12	63	85
17	18	13	20
18	41	20	25
20	21	52	81

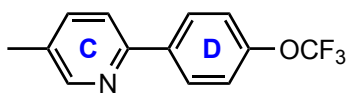


R =



CK-2-68

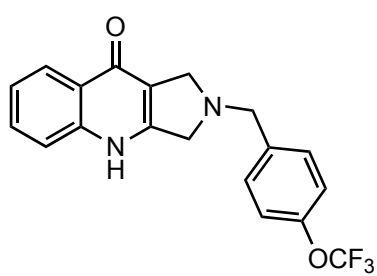
X = Cl

 $IC_{50}(3D7) = 31 \text{ nM}$ 

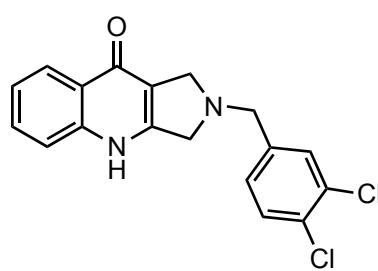
SL-2-25 (1)

X = H

 $IC_{50}(3D7) = 54 \text{ nM}$



IC_{50} (3D7) = 200 nM



IC_{50} (3D7) = 70 nM

